LASER COLLIMATION FOR LINEAR COLLIDERS

H. Aksakal, Nigde University, Nigde, Turkey
J. Resta-López, John Adams Institute, Oxford University, UK
F. Zimmermann, CERN, Geneva, Switzerland

Abstract

We explore the possibility of laser-based postlinac beam collimation in future linear colliders. A laser employed as a spoiler can neither be 'destroyed' by the beam impact nor generate collimator wakefields. In addition, the postlinac collimation section, presently the longest part of linear-collider beam delivery systems, can be shortened. In this paper we investigate different types of laser modes for use as spoiler. Suitable laser beam parameters and modes are discussed for collimation in both CLIC and ILC.

INTRODUCTION

The collimation system of future linear colliders should fulfil two main functions: reduction of the background in the particle detectors by removing beam halo particles, i.e., particles at large betatron amplitudes or energy offsets, and protection of machine components against mis-steered or off-energy beam pulses. The design of a collimation is not trivial, as it has to obey a number of often conflicting constraints: the system should not produce intolerable wakefields which adversely affect the beam stability or degrade the nominal luminosity, and it should withstand the impact of a full bunch train in a failure scenario. This last condition determines usually the length of the conventional collimation systems, which are based on spoilers and absorbers. Alternatively, following some pioneering studies [1], we here explore the viability of laser-based collimation in linear colliders. A laser collimation system could have the following advantages: a laser employed as a spoiler can neither be destroyed by the direct beam impact nor generate collimator wakefields. In addition, the postlinac collimation section could be shortened.

LASER COLLIMATION LAYOUT

Laser collimation consists in Compton scattering of electrons (positrons) in the transverse halo tails off a high power laser beam. The laser beam can enter the vacuum pipe through a dielectric material, and a 'quasi'-head-on collision between the electron beam and the laser beam may occur, as is illustrated in Fig. 1. We consider very small collision angles ($\theta_0 \sim \mu$rad).

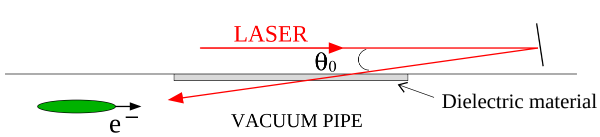

Figure 1: Schematic of the electron beam-laser collision region.

The energy distribution of the scattered electrons extends over a wide range. Figure 2 shows the energy spectrum of the unpolarized Compton cross section, $1/\sigma_c d\sigma_c/dy$ [2], as a function of the fractional energy of the scattered electron $E/E_0 = 1-y = 1-\hbar\omega/E_0$ (where $\hbar\omega/E_0$ is the scattered photon energy). This curve has been given for the value $x = 4E_0\hbar\omega_0/(m_e^2c^4) = 4.5$. If $x \geq 4.8$ pair production is possible and, therefore, this regime should be avoided.

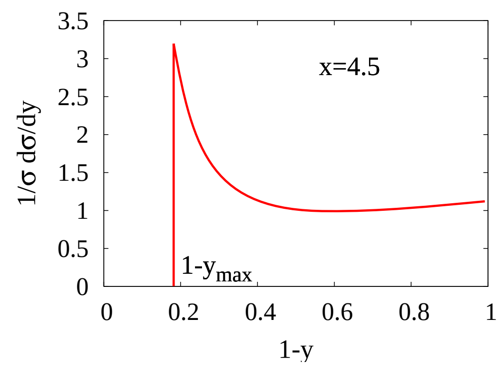

Figure 2: Energy spectra of scattered unpolarized electrons for x=4.5.

The scattered halo particles, which are off energy, would be intercepted by downstream absorbers placed in a region with nonzero horizontal dispersion D_x. As indicated in Fig. 2 the energy distribution of the scattered electrons peaks at the lower final energy of $\delta_c \approx 20$ %. The rms width of the distribution is of similar magnitude. The horizontal spot size of the scattered beam at a downstream absorber is approximately $\sigma_x \approx D_x\delta_c$, assuming that the dispersion is generated downsream of the laser-beam collision point. If θ_s denotes the average angle of the scattered electrons the vertical size at the absorber can crudely be estimated as $\sigma_y \approx R_{34}^{l\to A}\theta_s$, where $R_{34}^{l\to A}$ is the transport matrix element from the beam-laser collision point (l) to the absorber position (A). For example, if the dispersion is generated by a chicane of length L and no other elements exist between collision point and absorber, $\sigma_y \approx L\theta_s$.

In order to avoid the fracture of the absorber upon beam impact, the transverse density of the scattered beam must stay below a certain limit. Assuming Gaussian beams, this condition can be expressed as $N_s/(2\pi\sigma_x\sigma_y) \lesssim N_s/(2\pi\sigma_{r,\min}^2)$, with N_s the number of scattered beam particles, and $\sigma_{r,\min}$ the minimum rms transverse spot size at which absorber fracture does not yet occur for the incident beam intensity N_s, and depends on the material. This translates into the following constraint: $\sigma_x\sigma_y = D_x\delta_c L\theta_s \gtrsim \sigma_{r,\min}^2$.

Another constraint for the dispersion function and the length of the chicane comes from the tolerable emittance growth due to synchrotron radiation [3]: $\Delta(\gamma\epsilon_x) \simeq (4.13\times 10^{-8}\ \mathrm{m}^2\ \mathrm{GeV}^{-6})E^6 I_5$, where I_5 is a radiation integral ($I_5 \equiv \int \mathcal{H}/|\rho|^3 ds$; see [3]). In the case of CLIC, for example, $I_5 \approx 10^{-19}\ \mathrm{m}^{-1}$ is about the tolerable limit.

Laser modes for collimation

Our aim is to investigate appropriate laser modes for electron (positron) beam collimation. They should efficiently clean the transverse beam halo, while the impact on the beam core must be minimized. The laser beam spot size w (twice the rms size) is conventionally given by [4]:

$$w(s) = \sqrt{\lambda Z_R/\pi(1+s^2/Z_R^2)} = w_0\sqrt{1+s^2/Z_R^2}\ , \quad (1)$$

with λ the laser wavelength, Z_R the Rayleigh length, s the longitudinal variable, and $w_0 = (Z_R\lambda/\pi)^{1/2}$. In addition, the laser pulse energy is given by $A = I\tau_L\pi w^2 = P\tau_L$, where I is the intensity of the laser mode, τ_L the full laser pulse length, and P the peak power of the laser beam. The figure of merit is the conversion efficiency [2, 5]:

$$K_c = 1 - \exp(-k_c) = 1 - \exp\left(-\sigma_c \frac{I\tau_L}{\hbar\omega_0}\right)\ , \quad (2)$$

which depends on the incoming photon energy $\hbar\omega_0$ and the laser intensity I, and represents the probability that an electron (positron) in the beam will Compton scatter. The intensity I in Eq. (2) can be computed from the Helmholtz wave equation using an appropriate coordinate system. We have studied different types of laser modes which can fulfil the collimation requirements. The transverse collimation depth in units of the rms spot size σ is denoted by n. The target value for n is normally quite different in the two transverse planes, namely $n_y \gg n_x$. In order to obtain an efficient collimation we adjust the laser parameters so that $k_c(n\sigma) \approx 1$, which corresponds to a conversion efficiency $K_c \approx 0.63$. We have explored three possible laser mode scenarios for collimation, which are described in the following.

Hermite-Gaussian (HG) laser mode intensity:

$$I_{\ell m} = I_0 \frac{w_0^2}{w(s)^2} H_\ell^2\left(\frac{\sqrt{2}x}{w(s)}\right) H_m^2\left(\frac{\sqrt{2}y}{w(s)}\right) e^{\left(-\frac{x^2+y^2}{w(s)^2}\right)}\ .$$

A Hermite-Gaussian mode ($\ell = 1, m = 0$) was already considered in earlier laser collimation studies [1]. Another possibility here considered is the HG mode ($\ell = 1, m = 1$). As an example, Fig. 3 shows the corresponding coefficient $K_c(x,y)$ estimated for collimation in CLIC.

Laguerre-Gaussian (LG) laser mode intensity:

$$I_{\ell m} = I_0 \frac{w_0^2}{w(s)^2} \frac{2\ell!}{\pi(m+1)!} e^{-2\rho^2}(2\rho)^{|m|}[L_\ell^m(2\rho)]^2\ ,$$

where $\rho = (x^2+y^2)/w(s)^2$. Figure 4 shows the factor $K_c(x,y)$ for the LG laser mode ($\ell = 1, m = 1$). A hollow laser beam will scatter the particles with larger amplitude, while smaller amplitude particles (core) are not affected at all.

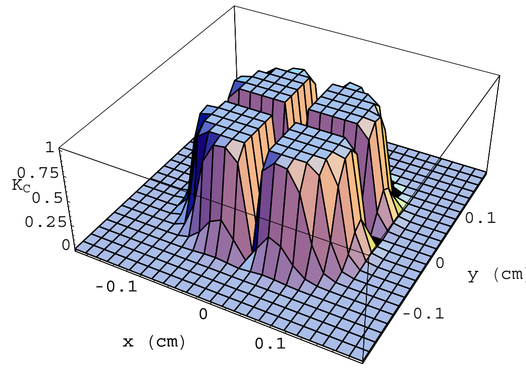

Figure 3: $K_c(x,y)$ using the I_{11} HG mode.

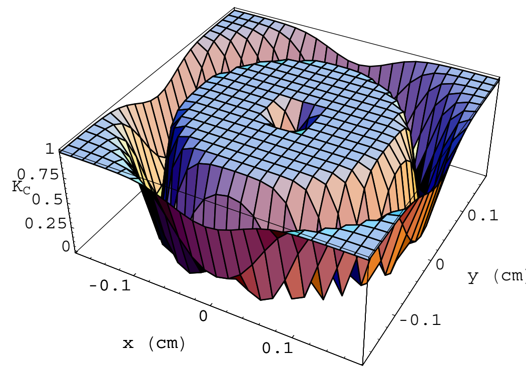

Figure 4: $K_c(x,y)$ using the I_{11} LG mode.

Bessel laser mode intensity: Another hollow laser beam for collimation can be created from Bessel laser modes. The intensity of this mode is

$$I_\ell(x,y,s) = I_0\cos^2(\theta)J_\ell^2(k_\perp r)\ .$$

where θ is the angle between two plane waves which produce the Bessel mode [6]. As an example, $K_c(x,y)$ for the Bessel mode $\ell = 1$ is shown in Fig. 5.

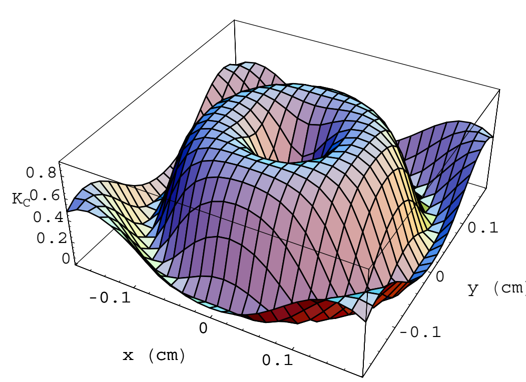

Figure 5: $K_c(x,y)$ using the I_1 Bessel mode.

As is known, the transverse profile of a Gaussian laser beam grows during propagation because of its inevitable diffraction characteristics, and this effect would weaken the efficient interaction of the electron and the beam laser beam, especially in the part of the interaction region which extends beyond the Rayleigh length. The Bessel beam may preserve its transverse distribution while it is travelling [4]. A Bessel beam can be obtained from a Gaussian laser beam by using an axicon which consists of a prism and a focusing lens. Radially and circularly polarized Bessel laser beams have longitudinal electric field components, which can accelerate or decelerate the electron beam. For collimation purposes, an azimuthally polarized Bessel beam should be used instead, which has zero longitudinal electric field. Another way to obtain Bessel beam is to use a combination of two incident electric plane waves with an incidence angle θ [6].

The transverse size of the laser beam can be tuned for optimum collimation using a mirror system. The horizontal and vertical beam size may be optimized by varying the two beta functions. The Rayleigh length Z_R in (1) is given by $Z_R = (4/\pi)\lambda F_N^2$, where F_N can roughly be defined as the ratio of the focal length to the diameter of the focusing mirror. We considered this kind of optical system for the case of HG and LG modes, denoting by d the distance between the mirror and the laser beam waist. For Bessel modes it is not necessary to use focusing mirrors to obtain the desired Rayleigh length.

The laser modes considered above are circularly symmetric, while the electron beam for linear colliders is flat ($\sigma_y/\sigma_x \ll 1$). Nevertheless, the betatron functions at the collimation point could be matched to perform simultaneously horizontal and vertical collimation using a single laser, in particular since the vertical collimation depth in units of σ_y, n_y, is typically about 10 times larger than the horizontal one, i.e. $n_y \approx 10n_x$.

APPLICATION TO ILC AND CLIC

Assuming the electron beam parameters of Table 1, we have calculated some example parameters for laser collimation in ILC and CLIC. Table 2 summarizes the results for the different modes considered in the previous section.

Table 1: Electron beam parameters for ILC and CLIC at 250 GeV.

parameters	**ILC**	**CLIC**
beam energy E [GeV]	250	250
$\gamma\epsilon_x/\gamma\epsilon_y$ [mm rad]	10/0.04	66×10^{-5}/10^{-5}
β_x^*/β_y^* [mm]	20/0.4	7/0.09
σ_z [μm]	300	30.8
repetition rate $f_{\rm rep}$ [Hz]	5	30
# particles/bunch	2×10^{10}	2.56×10^9
# bunches/pulse	2625	220
time separation of bunches in a train t_b [ns]	369.2	0.267
hor. coll. depth n_x [σ_x]	9.6	9
vert. coll. depth n_y [σ_y]	74	69
β_x/β_y [m] (at laser IP)	23.8/100	89/100

Table 2: Laser beam parameters.

laser collimation in ILC			
parameters	**HG**	**LG**	**Bessel**
mode (ℓ, m)	(1,1)	(1,1)	$\ell = 1$
power P [TW]	1.2	0.038	0.02
pulse energy [J]	2.84	0.0074	0.08
intensity I_0 [10^{16}W/cm^2]	3.5	0.0058	0.01
Rayleigh length Z_R [mm]	0.14	0.7	0.24
wavelength λ [μm]	23.6	95	91
F [cm]	5	15	-
F_N	1520	1033	-
d [cm]	0	0	-
Bessel θ [mrad]	-	-	0.9
τ_l [ps]	2.4	0.4	4
w_0 $[mm]$	32	0.145	83
# photons/pulse (10^{19})	1.4	0.22	0.04
laser collimation in CLIC			
parameters	**HG**	**LG**	**Bessel**
mode (ℓ, m)	(1,1)	(1,1)	$\ell = 1$
power P [TW]	0.4	0.4	0.12
pulse energy [J]	0.82	0.77	0.4
intensity I_0 [10^{17}W/cm^2]	0.75	0.082	0.13
Rayleigh length Z_R [mm]	0.115	8.15	0.12
wavelength λ [μm]	5	0.014	0.13
F[cm]	19	20	-
F_N	163	169	-
d [cm]	1	1	-
Bessel θ [mrad]	-	-	4.7
τ_l [ps]	2	5.6	2
w_0 [μm]	41	39	17
# photons/pulse (10^{18})	4.1	11	0.4

SUMMARY AND OUTLOOK

We have studied different laser modes to be used for beam collimation in future linear colliders. Hollow laser beams based on LG and Bessel modes offer the possibility to simultaneously collimate the transverse beam halo in all directions. Laser beam parameters for postlinac collimation in ILC and CLIC at 250 GeV beam energy have been calculated. In principle, the parameters are within the reach of present laser technology. Nevertheless, further studies are needed on the detailed optical system, laser stabilization and laser failure scenarios.

REFERENCES

[1] F. Zimmermann, SLAC-PUB-7883, 1998.

[2] V. Telnov, NIM A**355** (1995) 3.

[3] R.H. Helm, *et al.*, IEEE Tr.N.Sc. 20, 900 (1973).

[4] Dazhi Li, *et al*, J. Nuclear Science and Thecnology, Vol. 40, No. 8 (2003) 579.

[5] H. Aksakal, et al., NIM A**576** (2007) 287.

[6] T. Grosjean, and D. Courjon, Optics Express, Vol. 14 (2006) 2203.

